the non ordered part of the polycrystalline sample which can be associated to the crystallographic grain surface.

Hence, our measurements suggest that the origin of the MR at $T<T_C$ characteristic of the granular behaviour is the not fully saturate FM order at the boundaries of the crystallographic grains. However, when neighbouring grains are crystallographically well aligned, as is the case of the epitaxial film of LCMO on MgO, the magnetic state at the gain boundaries is more easily turned to FM alignment.

The values of the MR attained by polycrystalline films at low temperatures under high magnetic fields are rather large (≈70%) compared to those of the epitaxial films (≈20%). However, from the magnetic point of view they display similar saturation magnetisation at 4K. The latter indicates that few regions in the sample, which give very little contribution to the magnetisation control the electrical transport in polycrystalline samples at 4K. In this sense, such behaviour recalls the electrical transport in percolative systems.

The total resistance in a percolative system is determined by the lowest resistive percolative path. In addition, the total resistivity of the path can be determined by the behaviour of the grain boundaries, but as magnetisation is a volume measurement, it would reflect the behaviour of the volume material.

The existence of MR at temperatures below T_C can be associated to a non fully FM ordered GB. And the reason of the large magnetoresistance in polycrystalline films can be attributed to the nature of the DE interaction which is a first neighbours interaction.

At low temperature, polycrystalline films display localisation phenomena which give rise to an upturn of the resistivity upon cooling and the resistivity has been found to be less dependent on the applied magnetic field than at higher temperatures. In addition, it has been observed the existence of a large MR at low magnetic fields in granular films. The relationship between these phenomena will be discussed in the following section

3.2.3 Low Field Magnetoresistance and Low temperature localisation

3.2.3.1 Low field magnetoresistance

Low field magnetoresistance (LFMR) is the change of the resistivity for low applied magnetic fields of the order of the coercive field.

LFMR appears in polycrystalline films and powders of manganites exhibiting the FM/M to PM/I transition and the magnetic field associated to it is of the order of H_C.

LFMR is defined as:

$$\%LFMR = \frac{\rho^{max} - \rho^{*}}{\rho^{max}} \qquad \textbf{Eq. 3-2}$$

where ρ^{max} is the maximum of resistance (at H_C) and ρ^{*} is the high fields extrapolated resistivity (Fig. 3-38).

Our measurements show that LFMR rapidly decreases with temperature, and that it disappears below T_C (Fig. 3-39). In addition, LFMR drops faster than M^2 (Fig. 3-39) which does suggest that it does not direct spin dependent electron tunneling between the grains [70]. It could be associated to a loss of spin polarisation or to inelastic tunneling.

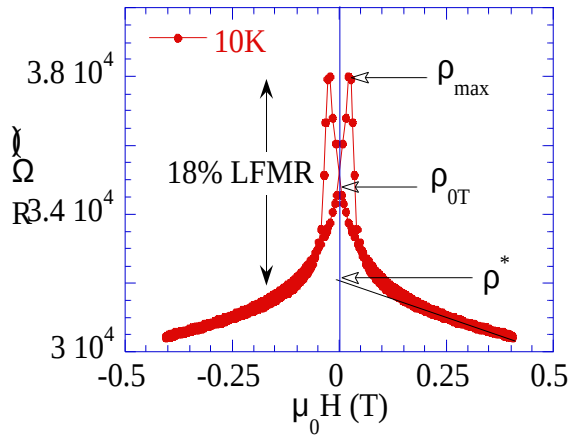

Fig. 3-38 ***Hysteresis of the R(H) isothermal measurements in polycrystalline films***

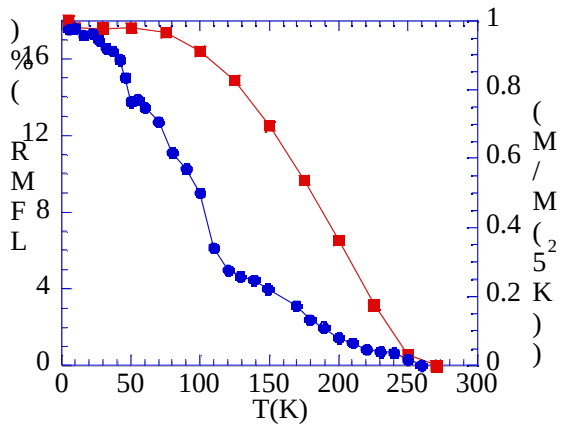

Fig. 3-39 ***Thermal evolution of the LFMR in a polycrystalline LCMO film on MgO***

In Fig. 3-40 is displayed the LFMR and the grain size of the films as a function of the substrate temperature. It is observed that LFMR is only measurable in polycrystalline films and it is absent in epitaxial films.

In addition, our results suggest that there is no direct relationship between grain size and LFMR in the range of grain size of our study. However, in the small grain size region of polycrystalline films, the LFMR diminishes as the grain size rises.

From the above measurements we conclude that the granular behaviour in the manganites does not scale with the grain size for grain sizes below 0.2μm. Dubourdieu et al. [96] argued that the LFMR

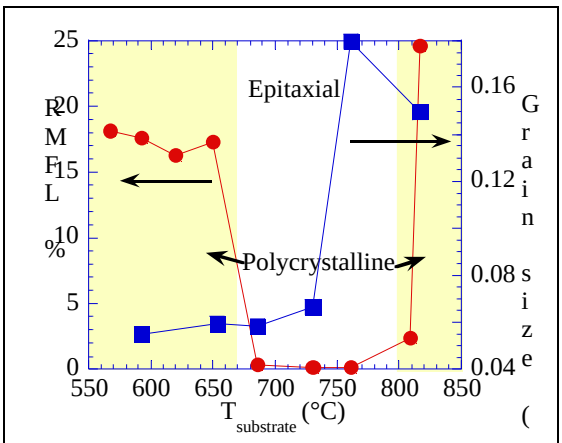

Fig. 3-40 ***Evolution of the LFMR and the grain size in LCMO films on MgO with the substrate temperature.***

was grain size independent in the range of grain sizes between 20nm to 100nm in agreement with our data.

In conclusion, our studies suggest that LFMR depends on the crystallographic misalignment of the grains and not on the grain size. The main reason is that epitaxial films on MgO are certainly also constituted by grains but the grains are crystallographically well oriented and no evidence of LFMR has been observed in these films. In addition, polycrystalline films deposited at high substrate temperatures have large grain sizes and exhibit large LFMR.

In this section, we have found that polycrystalline samples are highly FM saturated at temperatures about 4K. Hence, the upturn of the resistivity at lower temperatures is associated to phonon assisted tunnel. Next section will be devoted to the understanding of the low temperature localisation.

3.2.3.2 Low Temperature localisation

The upturn of the resistivity below 20K has also been observed in several systems as for example bulk granular powders [98] with grain size below 30nm and on LSMO films on bicrystalline $SrTiO_3$ substrates [78]. The former authors attribute the low temperature localisation to Coulomb effects appearing only for small grain sizes, and they deduce from their data that there exist a dead layer at the surface of the grains which increases in thickness when reducing the grain size. The latter authors did not give any explanation, and it can not be understood on the basis of their MMR mesoscopic model tunnel junctions [99] as well as in ramp-edge junctions [100] a slight upturn of the resistivity at low temperatures is observed through certain junctions which exhibit non Ohmic behaviour while others just exhibit the broad peak in the resistivity of the junction at temperatures below T_C, but when measuring the films in the plane no evidence of the broad peak is observed [73]. Hence, these observations suggest that the low temperature localisation and the broad peak of the resistivity at temperatures below T_C are created by different phenomena and are both related to the existence of GBs.

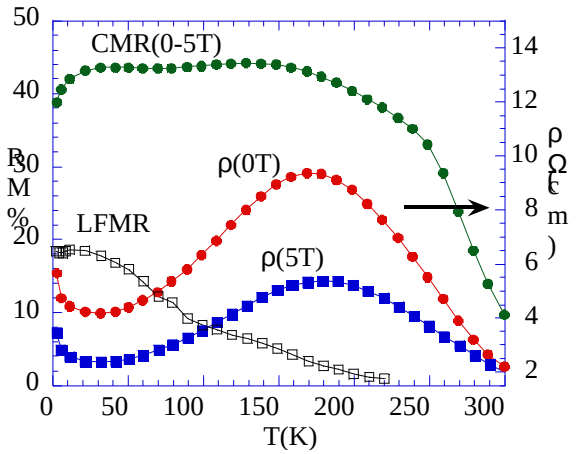

Fig. 3-41 *Magnetotransport measurements on a 30nm thick polycrystalline LCMO film on MgO substrate.*

In Fig. 3-41 are shown the magnetotransport measurements on a film of 60nm of LCMO on MgO deposited at low temperature (567°C). The residual resistivity is large, around 4Ωcm which is several orders of magnitude higher than in a single crystal (140μΩcm).

In order to understand the origin and characteristics of the low temperature localisation we have performed a series of resistivity measurements in the low temperature regime (T<15K) with high applied magnetic fields (0-7T) and in another series of measurements for low applied magnetic fields (0-0.5T) with the four contacts technique.

The low temperature resistivity can be rather well fitted for temperatures below 15K with an activation law $\rho = \rho_0 \exp\left(\frac{E_a}{k_B T}\right)$ (Fig. 3-42). In this range of temperatures, the simple activated law fits better the experimental data than $\rho \quad \exp\left(\frac{\Delta}{k_B T}\right)^{\frac{1}{2}}$ that could be attributed to Coulomb Blockade effects.

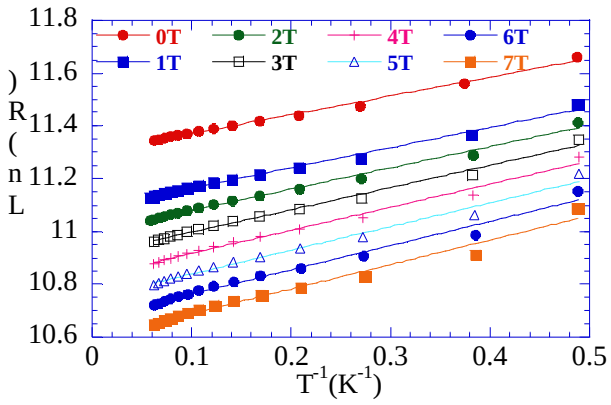

Fig. 3-42 ***Fit with an activated law of the low temperature resistivity upturn***

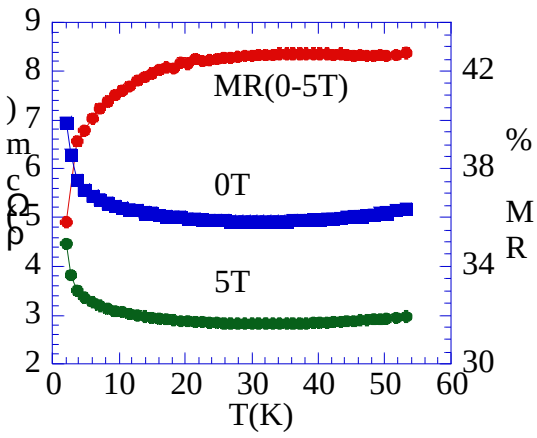

Fig. 3-43 ***Evolution of the magnetotransport at low temperatures exhibiting the decrease of the MR when the localising effects sets in.***

The activation energy is not found constant with the applied magnetic field and it ranges from 60μeV to 80μeV for the highest fields. Thinner films exhibit a more marked low temperature localisation and activation energies of about 179μeV have been measured. The obtained value for the activation energy is around 0.7K to 0.9K in a 60nm thick film and 1.7K in a 30nm thick film, are comparable to the thermal energy in this range of temperatures.

The dependence of the energy barrier on the magnetic field could be an indication that spin dependent tunneling or hopping through a magnetic barrier is the electronic process governing the charge transport at low temperatures.

The low temperature localisation has been often associated to magnetocoulomb effects. However, a simple activated law seems to fit better the experimental data. In addition, Coulomb Blockade effects may give an enhancement of the magnetoresistance [101], which is not present in our polycrystalline samples. At low temperatures, when the localising effects appear, the high field magnetoresistance decreases as shown in Fig. 3-43. However, further research is needed to rule out Coulomb blockade effects which can happen concomitantly with other mechanisms.

Low temperature measurements

To go further in the understanding of the low temperature localisation present in granular films, a series of transport measurements at low (2K) and very low temperature (30-200mK) have been performed on a 60nm thick LCMO film on MgO deposited at low substrate temperature (585°C).

In previous section, we have concluded that the low temperature upturn is sensitive to the applied magnetic field but less sensitive to the applied magnetic field than the mechanism creating the high field MR at higher temperatures.

We have first used the four point contact method to perform the V(I) curves on the granular film. The four probe method used to measure the V(I) curves consists in four metallic retractable needles (Fig. 3-44). A continuous current is injected in the side contacts and the voltage is measured in the central ones.

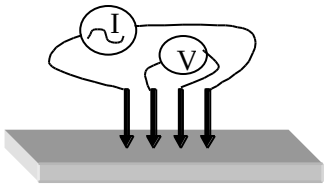

Fig. 3-44 *Schematic representation of the four point contact method used for transport and V(I) measurements.*

At low temperatures the V(I) measurements show that there exist a non linearity in the V(I) curves. At 1.9K there is a clear change of slope at 0.029mA (Fig. 3-45) which is symmetrical in terms of current. The value of the voltage for the value of the injected current at which the change of slope takes place is 3.24V in both cases. For higher current, there is no evidence of heating up the sample when increasing the current injection. The calculated power dissipation at the slope change point is 93µW.

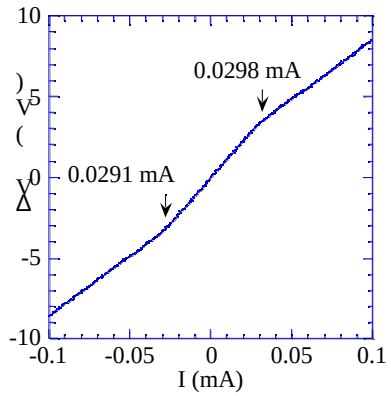

Fig. 3-45 *V(I) curve at 1.9K displaying non linear effects.*

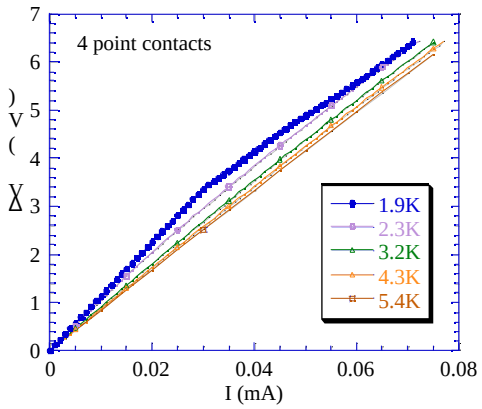

Fig. 3-46 *V(I) curves in the temperature range between 1.9K to 5.4K*

Considering the granular sample as a percolating system, in the localised regime, all the current could pass through narrow paths which could locally increase the temperature thus making the resistivity at this point decrease. Nevertheless, if such phenomena happened in our samples the change of slope would be progressive which is not the case (Fig. 3-45)

The anomalies in the V(I) curve appear at around 2K as shown in Fig. 3-47 and under the application of a external magnetic field (Fig. 3-48) the anomalies on the V(I) curves have a tendency to appear at higher values of the injected current.

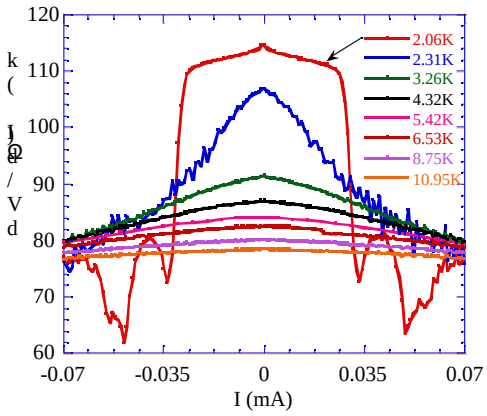

Fig. 3-47 *Apparition of non linearities in the V(I) curves with temperature.*

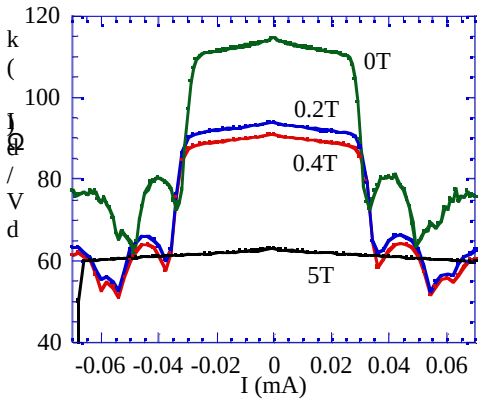

Fig. 3-48 *Effect of an applied magnetic field on the V(I) characteristics at 2K.*

In order to rule out rectifying problems associated to point contacts, we have repeated the experience but using four stripes of silver paste as contacts as shown in Fig. 3-49. dV/dI measurements at 1.9K are displayed for the silver paint contacts performed at different applied magnetic fields (Fig. 3-50). The 0T curve shows similarities with the four point contact measurements (Fig. 3-47).

Similar behaviour is observed using both types of contacts and the anomalies in the dV/dI curves occur at similar injected currents (Fig. 3-51). Hence, the change of slope is not an artefact of the measurement. If they are due to tunneling through a barrier, the sample contains so many grains that percolation through a path without GB is impossible.

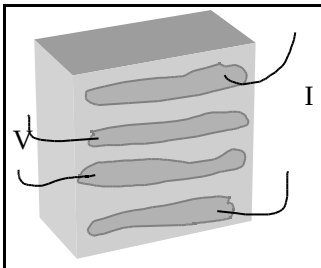

Fig. 3-49 *Schematic representation of the four silver paste contacts for the V(I) measurements*

Non linearities in I(V) curves can be associated to tunneling processes. The existence of a magnetically disordered GB may represent a energetic barrier which can be crossed by thermal activation at high temperatures.

These measurements show that the non linearities in the V(I) curves appear at low temperatures (2K), which are comparable to the energy barriers obtained. The non linearities are sensitive to the applied magnetic fields, so the tunneling barrier should be magnetic.

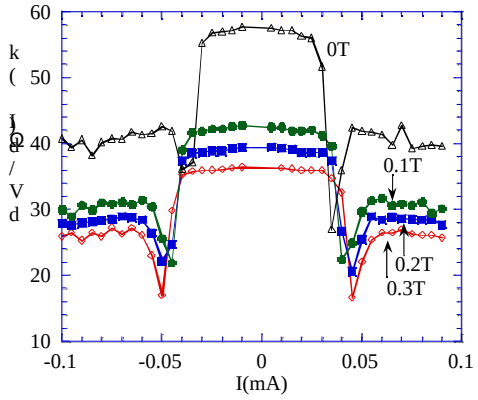

Fig. 3-50 *dV/dI characteristics for different applied magnetic fields using silver paste contacts.*

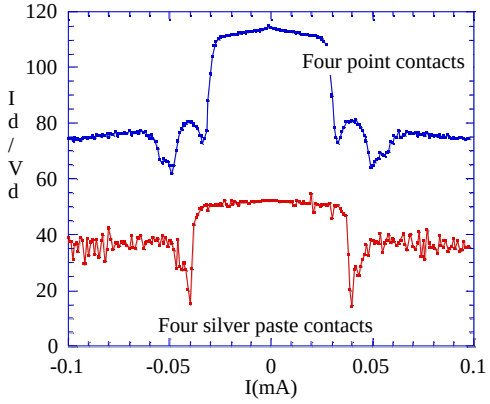

Fig. 3-51 *dV/dI characteristic curves at 1.9K obtained at zero applied magnetic field and using different measurement set-up.*

Regarding the basis of the tunneling mechanism that could be taking place between the grains, it is not easy to extrapolate Simmons equations [69] to a case where the current is injected. For that reasons we performed I(V) measurements at lower temperatures (mK) where activated phenomena may be supressed. In a tunnel barrier the dependence of the dI/dV on the applied voltage is, in first approximation and for low applied voltages, proportional to $a+bV^2$. So if tunneling is taking place between the grains a parabolic function should be obtained when measuring the changes in the tunneling current as a function of the applied voltage. (section 2.2.4).

I(V) measurements at very low temperatures (T≈30mK)

The same sample investigated in the previous section has been used to perform I(V) measurements at very low temperatures (≈mK). A series of µ-contacts have been performed to the sample (Fig. 3-52). The aim of the µ-contacts disposition is to check if transport is done by percolating paths.

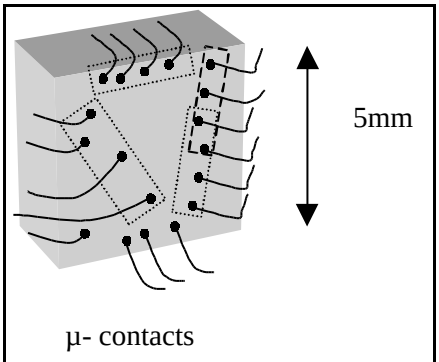

Fig. 3-52 *Schematic representation of the µ-contacts distribution on the polycrystalline LCMO film on MgO.*

The I(V) measurements were performed using a sequence of voltage pulses with the same pulse time application than time interval between them (t). This method was chosen to reduce possible heating up processes.

I(V) measurements at 30mK are shown in Fig. 3-53. The I(V) characteristics were performed for the different groups of contacts labelled in the Fig. 3-52. All the contacts measured display non linear I(V) characteristics at very low temperatures and their specific behaviour depends on the group of contacts selected.

Hence, this result corroborates that transport in granular films is inhomogeneous. In four of the contacts, the current increases progressively with the applied voltage. However, in the other one (3-4-7-8), the system is blocked and the current can only flow after crossing a limiting voltage. This behaviour is normally associated to Coulomb blockade phenomena. In the case of Coulomb Blockade, a stair shaped I(V) characteristic would be expected.

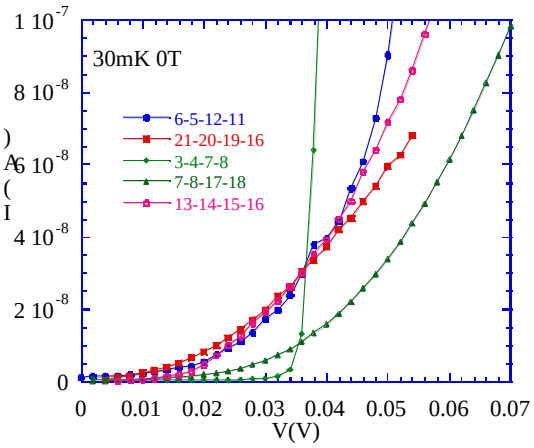

Fig. 3-53 *Non linear I(V) at 30mK for several groups of contacts labelled in the figure.*

Several transport processes can take place in a system composed by a insulating barrier between two metallic electrodes:

i) direct tunneling from one electrode to the other,

ii) Tunneling through localised states in the barrier and resonant with the electrons at the Fermi level of the electrodes.

iii) phonon assisted tunneling

iv) phonon assisted tunneling through localised states in the barrier. In this phonon assisted tunneling, Coulomb blockade effects can take place due to charging of the particle or magnetic ion receiving the tunneling electron.

The different mechanisms differ in their thermal evolution and on the barrier thickness and voltage dependence. Direct or resonant tunneling through localised states in the barrier are temperature independent. In addition, in direct tunneling the conductance depends exponentially on the double of barrier thickness, while in resonant tunneling through localised states in the barrier the conductance depends exponentially on the barrier thickness.

Analysis of the I(V) curves: Tunneling processes

Several mechanisms seem to take place in electrical transport on the present manganite granular system because the system is inhomogeneous.

In a percolating system, one barrier can determine the global behaviour of the path and thus the mechanism controlling the transport in this GB will determine the whole electrical conduction in the path. In the following we will identify these mechanisms in the measurements performed on different contacts and thus on different paths.

Contacts 7/8/7/18

The series of contacts labelled 7/8/17/18 presented a I(V) characteristics as shown in Fig. 3-54. Under the application of a magnetic field, the curve shifts towards higher values of the current. The value of the conductance, of the order of $1.5*10^{-6}\ \Omega^{-1}$, is less than the quantum limit ($\approx e^2/\hbar \approx 2.4*10^{-4}\Omega^{-1}$) which corresponds to the minimum value of the conductance for a thin wire or a neck constriction, so the electrical conduction mechanism is a tunneling one.

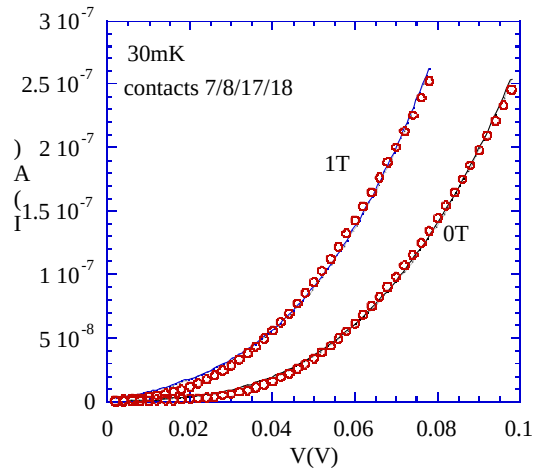

Fig. 3-54 *I(V) characteristics at 30mK for the contacts labelled 7/8/177/18 for 0 and 1T of applied field .*

The I(V) characteristics for low voltages follows the behaviour deduced by Simmons for tunnel junctions with a rectangular barriers approximation [102]:

$$J = \beta\left(V + \gamma V^3\right) \qquad \textbf{Eq. 3-3}$$

where:

$$\beta = \frac{3}{2} e^2 \frac{(2m\varphi)^{1/2}}{h^2 s} \exp\left(A\varphi^{1/2}\right) \; ; \; \gamma = \left[(Ae)^2 / 96\varphi\right] - \left[(Ae^2) / 32\varphi^{3/2}\right] \qquad \textbf{Eq. 3-4}$$

and A is defined in Eq. 2-6 (section 2.2.4). Hence, $dI/dV = a + bV^2$.

In Fig. 3-55 the fit is shown for positive and negative values of the applied voltage in the 3/4/7/8 contacts at a temperature of 200mK with and without applied field which confirms the tunneling transport at low temperatures. The measurements are quite symmetrical. However, often the dI/dV curves deviate strongly from the nearly parabolic behaviour close to the 0 bias voltage as is the case when tunnel junction have dissimilar FM electrodes. The presence of metallic particles, magnons, magnetic impurities, localisation effects, multi-step tunneling and states in the barrier or at the interface can affect the spin polarisations of the tunneling electrons by causing spin flip scattering and a dip in the conductance at V=0 at low temperature can be expected to be due to some combinations of these effects as pointed out by Moodera et al. [60]

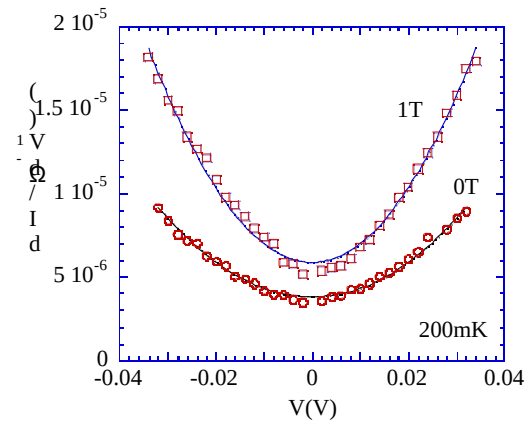

Fig. 3-55 *dI/dV characteristics at 200mK for the contacts labelled 3/4/7/8*

As we are unable to determine the current density because we ignored the width of the paths, we used the formula given by Simmons:

$$I = a\left[V + \left(\frac{0.0115\, s^2}{\varphi} - \frac{0.0315\, s}{\varphi^{3/2}}\right) V^3\right] \qquad \textbf{Eq. 3-5}$$

and including the effect of the image force:

$$I = a\left[V + \frac{0.0093\left(s - \frac{7.2}{\varphi}\right)^2}{\varphi - \frac{10}{s}} - \frac{0.0286\left(s - \frac{7.2}{\varphi}\right)^3}{\left(\varphi - \frac{10}{s}\right)^{\frac{3}{2}}}\right] \qquad \textbf{Eq. 3-6}$$

In order to obtain the *a* parameter, Simmons suggested to fit the linear zone of the I(V) curve for very low voltages. And, for higher voltages, the *s* (barrier thickness) and φ (barrier height) parameters can be fitted.

For 7/8/17/18 contacts at 0T the obtained value for the *a* parameter is 6.1 10^{-8} A/V and assuming that the grain boundary thickness is about 20Å as estimated in [98, 103], the calculated barrier height is of 0.47 eV at 20mK which is of the same order of magnitude than the value of the barrier height obtained in manganite base tunnel junctions using $SrTiO_3$ insulating layer [99] (band gap calculations gave 3 eV for the insulating gap in $SrTiO_3$).

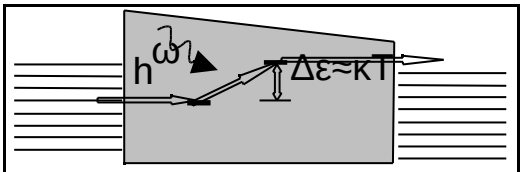

Fig. 3-57 *Schematic representation of phonon assisted inelastic hopping through two localised states in the barrier.*

The use of Simmons equation in this range of applied voltages is justified by the fact that the applied voltage is smaller than the barrier height.

Contacts 21/20/19/16

For another group of contacts 21/20/19/16, the I(V) characteristics are also well fitted with Simmons formula given above (Fig. 3-56). As the temperature is raised, the resistance of the path diminishes. At 30mK, the *a* parameter is estimated from the low voltage and assuming the barrier thickness to of 20Å, the barrier height is about 0.45 eV (close to the value obtained in the case of the 7/8/17/18 contacts).

Tunneling through localised states in the barrier

Under the application of a magnetic field, Simmons approximation did not allowed to satisfactorily find the barrier characteristic from the I(V) curves. A more complicated model has to be proposed.

Under an applied magnetic field, another mechanism adds to direct tunneling. In this sense, we recall that in tunnel junctions with amorphous silicon barrier when the barrier thickness was increased, the conductance showed different temperature and voltage dependence than the expected from direct tunneling. The value of the barrier height calculated from the transport measurements was too small. Such discrepancies were attributed to the existence of another process which takes into account the presence of localised states in the barrier. In such tunnel junctions the dominant conduction mechanism crosses over as a function of the barrier thickness from direct tunneling to resonant tunneling to directed hopping along quasi-one-dimensional chains of localised states, and in the bulk limit, to variable range hopping.

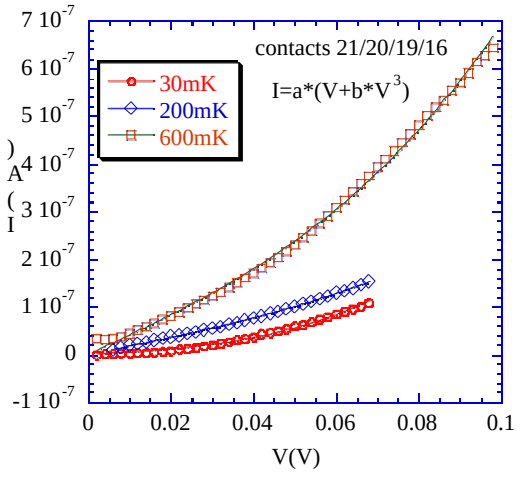

Fig. 3-56 *Thermal evolution of the I(V) curves measured for the group of contacts 21/20/19/16.*

The presence of localised states in the barrier allows the possibility of transferring electrons from one electrode to the other by other mechanisms than direct tunneling. Elastic contribution to resonant tunneling through localised states is often masked by phonon assisted inelastic hopping. Physically inelastic chains dominate the elastic resonant chains because the probability of finding aligned localised states in the barrier is low. In Fig. 3-57 phonon assisted inelastic hopping through two localised states in the barrier is sketched.

Conductance in such system depends on temperature as $(kT)^{4/3}$ for kT>>eV as reported by Xu et al.[104]. The authors deduced that inelastic hopping conductance becomes exponentially larger than the elastic-tunneling conductance as the barrier thickness increases:

$$\sigma_2^{hop} \quad \sigma_1^{res} (kT)^{4/3} \exp\left(\frac{4\alpha d}{3}\right) \qquad \textbf{Eq. 3-7}$$

where *d* is the barrier thickness and α is the inverse of the localisation length. As the temperature or the barrier thickness increases, the dominant conduction channel crosses over to hopping along chains containing a progressively larger number of localised states(>2). The obtained variation of the conductance for a junction containing N localised states was estimated to be:

$$\frac{\sigma_N^{hop}(T)}{\sigma_1^{res}} \quad (kT)^{N-1} (kT)^{\frac{N-1}{N+1}} \exp\left(\frac{N-1}{N+1}\alpha d\right) \qquad \textbf{Eq. 3-8}$$

The total conduction of the junction is the addition of the conductance due to direct tunneling, resonant elastic tunneling, and conduction to inelastic hopping through localised states. When increasing the temperature, the dominant channel in the inelastic hopping through states in the barrier shifts from 2 to 3 to 4 states.

For eV>>kT the dependence of the conductance with the applied voltage becomes

$$\sigma_2^{hop} \quad \sigma_1^{res} (eV)^{4/3} \exp\left(\frac{4\alpha d}{3}\right) \qquad \textbf{Eq. 3-9}$$

and the dependence with the number of states in the barrier is equivalent to equation Eq. 3-8 after the change of kT by eV.

Hence, we used a function like $I= aV+bV^{n+1}$ to fit our data because in our case eV>>kT (600mK=0.05meV). *n* parameter should give an average of the number of localised states (N) generating the hopping through the barrier. From the Eq. 3-8 we observe that the parameter n= N-1+((N-1)/(N+1)).

In Fig. 3-58 is displayed the I(V) measurements at 30mK for the 13/14/15/16 contacts at 0T and 1T. Two fits are performed: Simmons direct tunneling approximation (discontinuous line) and inelastic hopping through localised states in the barrier (continuous line). In the low applied voltages, the latter approximation fits better our experimental data.

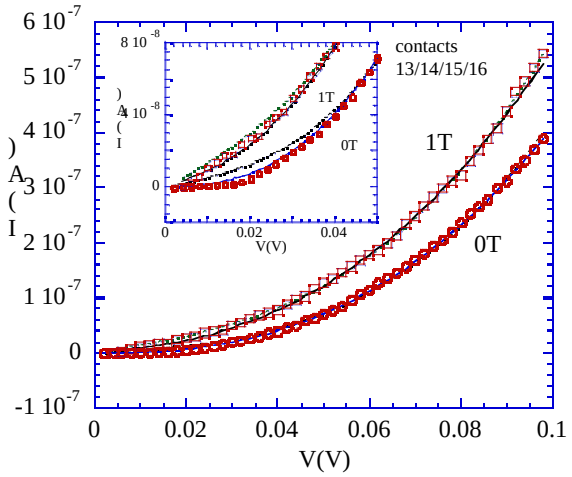

Fig. 3-58 *Fit of the I(V) curves at 0T and 1T of applied field using Simmons formula for direct tunneling (discontinuous line) and inelastic hopping formula through localised states (continuous line)(30mK)*

The experimental value of the averaged number of localised states in the barrier obtained from the fits at 0T and 1T are N=2.2 and 1.6 respectively.

That means that if hopping through the barrier takes place via localised states in the barrier. The application of a magnetic field increases the number of available localised states. In Fig. 3-59 is displayed the evolution of the number of localised states in the barrier, N, as a function of the temperature for two group of contacts. The results agree with the fact that when increasing the temperature the contribution of channels with more states in the barrier increases.

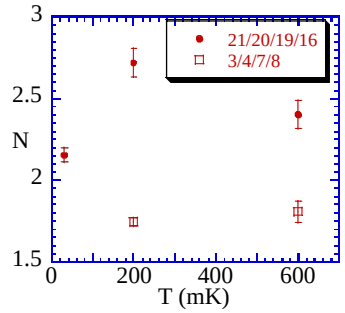

Fig. 3-59 *Experimental value of the averaged number of localised states in the barrier obtained from the fits at 0T and 1T*

Analysis of the I(V) curves: Evidences of Coulomb Blockade

At 30mK, the set of contacts (3/4/7/8) presents in the I(V) characteristics an anomalous behaviour (Fig. 3-60). The anomalous behaviour does not disappear under the application of an external magnetic field and is reproducible (Fig. 3-61). This behaviour is very similar to the expected behaviour in the case of Coulomb blockade. For applied voltages below a certain value, little current flows in the sample and above the limiting voltage value, current flows.

Coulomb blockade effects describe the inhibition of the charge transfer due to charging effects on a small particle [105, 106]. Tunneling do not take place until the electrostatic energy, eV (V being the applied voltage), is larger than E_C which corresponds to the energy cost for introducing a new

charge in the particle ($E_C=e^2/(2C)=e^2/2\varepsilon\varepsilon_0 4\pi r_a$ where C is the capacitance of the grain and r_a is the radius of the small particle).

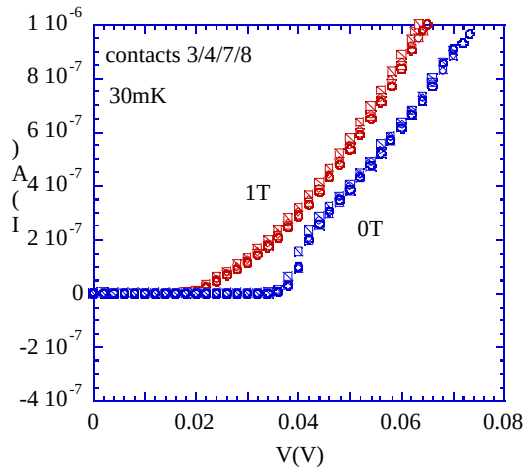

Fig. 3-60 *Blocking effects at 30mK in the 4 probe contacts 3/4/7/8.*

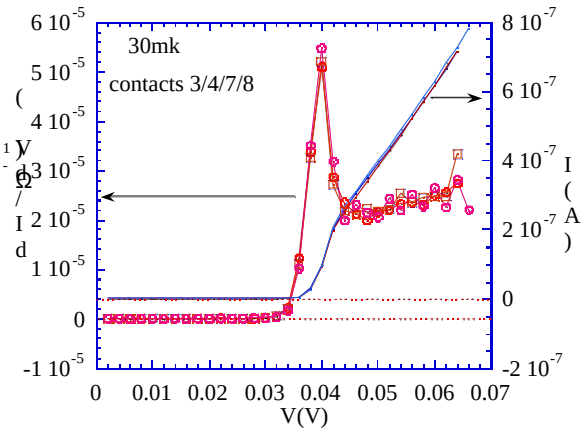

Fig. 3-61 *Repeated measurements at 30mK performed on the group of contacts displaying blocking effects. the behaviour is very reproducible.*

Coulomb blockade effects [70, 105] have been theoretically predicted in systems composed by one small metallic island separated from two metallic electrodes by two tunneling barriers (Fig. 3-62). The behaviour when there exist a effective Coulomb gap consist in periodic step like structure in the I(V) curves, each step corresponding to the addition of one electron into the small particle. The first step corresponds to a voltage of E_C/e while the following are equally spaced by 2 E_C/e.

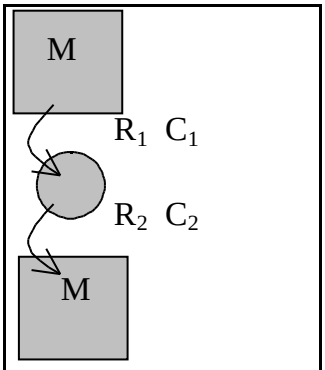

Fig. 3-62 *Coulomb blockade process.*

In order to observe the Coulomb gap, the thermal energy, kT, should not exceed the Coulomb gap energy E_C. When the Coulomb blockade is strong, sequential tunneling is replaced by cotunneling via a virtual state in the grain when increasing temperature. Sequential tunneling and cotunneling can be identified by the temperature dependence of the tunneling resistance. While the former shows an activated dependence with temperature, cotunneling depends linearly on $(E_C/KT)^2$. Cotunneling has been observed on ferromagnetic tunnel junctions [101].

In our measurements, when increasing temperature the blocking effects disappear giving rise to parabolic I(V) curves (Fig. 3-63). However, at 30mK and 0T the step in the I(V) curve appears at 40mV of applied voltage so E_C=40meV. This value of E_C is very close to the value obtained in ultrasmall cobalt clusters immersed in Al_2O_3 [106]. From the experimental value of E_C the blocking

particle radius corresponds to 3nm when supposing a spherical particle. This value is very close to the estimated value of the grain boundary thickness in films grown on bicrystals [103] and on powders [98].

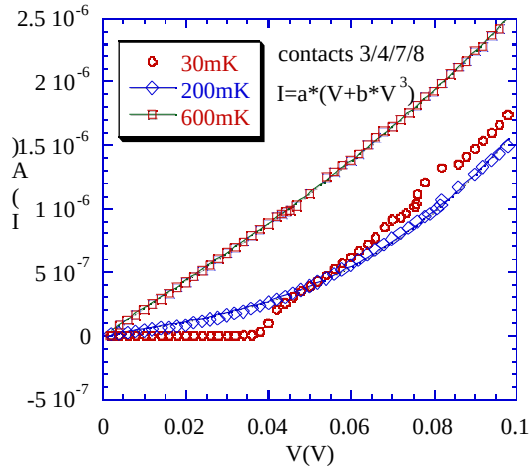

Fig. 3-63 *Effect of temperature on the evolution of the blocking effects on the same group of contacts.*

The effect of a magnetic field on a Coulomb blockade system composed by a double FM tunnel junction having as middle electrode a small particle exhibiting charging effects have been theoretically studied by Barnas et al.[105]. No change is expected on the barrier energy, E_C, but on the current at the step. Hence, oscillations in the tunneling magnetoresistance are expected with the same frequency as the steps in the I(V) curves.

Under the application of a magnetic field, in our films, the I(V) curve still displays the blocking effects (Fig. 3-60). The behaviour observed in our measurements do not correspond to the behaviour reported by Barnas et al. so suggesting that our system is not purely tunneling through ferromagnetic electrodes to one small grain exhibiting charging effects. In our measurements, the application of a magnetic field shifts the Coulomb barrier energy, E_C, to lower value (Fig. 3-60).

Lower Coulomb energy corresponds to a larger particle size (E_C=20meV corresponds to a particle radius of 6nm). A possible explanation is to consider that the application of the magnetic field aligns the electrodes to the central electrode that can consist in a cluster of Mn ions weakly exchange coupled to the neighbouring Mn. Therefore, the application of an external magnetic field permits these Mn ions to polarise their surroundings and increase the effective size of the ferromagnetic central electrode. The obtained value of the particle size is of the same order of magnitude as the grain boundary thickness of 2nm as pointed out by several authors.

When considering the above model, our measurements agree with grain boundaries larger than 6nm for grains of about 50nm of diameter in the current direction.

In addition, another characteristic signature of Coulomb blocking effects is the apparition of other anomalies in the I(V) curve for applied voltages proportional to the value of the voltage of the first anomaly. In the case of the measurement performed at 0T the second anomaly should appear at voltage around 0.12V and we did not perform the measurement up to such voltages to avoid heating effects. Nevertheless in the measurement performed at 1T, the second anomaly in the I(V) curve is expected at 60mV. In Fig. 3-64 are shown several measurements performed at 1T, all of them exhibit a

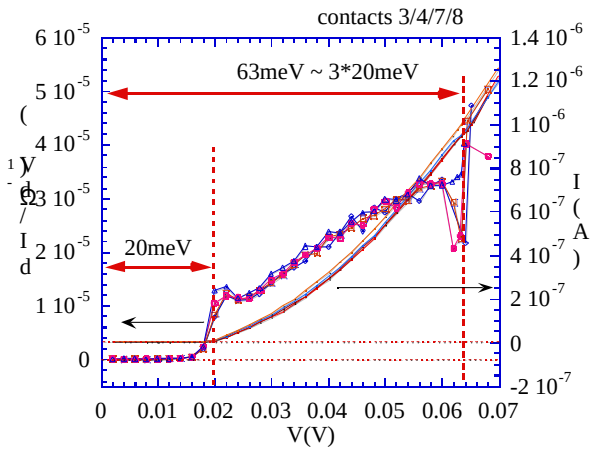

Fig. 3-64 *Blocking effects under 1T of applied magnetic field exhibiting the characteristic step like behaviour.*

second anomaly at an applied voltage of 63mV. Such anomaly is more clearly evidenced in the dI/dV numerical derivative (Fig. 3-64).

The above features agree with magnetocoulomb effects due to charging effects. However, surprisingly when comparing the thermal energy to the energy barrier, magnetocoulomb effects were not expected to disappear at 200mK. A possible explanation is that upon warming, new paths or tunneling transport mechanism can be added.

3.2.3.3 Conclusions from I(V) low temperature measurements

From the low temperature I(V) measurements, we conclude that transport in polycrystalline LCMO films on MgO(001) substrates is highly inhomogeneous. The electrical conduction being controlled by percolative paths, the behaviour of the most resistive GB in the path determines the behaviour of the whole electrical path. In addition, the inhomogeneity is probably also present in epitaxial LCMO films on MgO but percolative paths with well connected grains can give rise to a metallic and single crystal like resistivity behaviour.

The existence of a magnetic energy barrier is at the origin of the low temperature localisation. The application of an external magnetic field has been found to reduce the energy barrier.

We have identified different possible origins for the process governing the electrical transport at low temperatures. Inelastic hopping or tunneling through localised states in the barrier have been found to reproduce rather well our I(V) curves in some of the contacts.

In addition, magnetocoulomb blocking effects have been observed at 30mK in one group of contacts, consistent with a barrier width of 6nm and with a blocking energy of about 40meV. Coulomb energy is reduced under the application of a magnetic field of 1 Tesla to 20meV.